DOI: 10.13671/j.hjkxxb.2024.0116
冉毅媛,李学先,李玲, 等.2024.模拟降雨下土壤中黄钾铁矾对锑的固持效应研究[J].环境科学学报,44(9):347-355
RAN Yiyuan, LI Xuexian, LI Ling, *et al*. 2024. Antimony retention characteristics of jarosite in soil under simulated rainfall [J]. Acta Scientiae Circumstantiae, 44(9): 347-355

模拟降雨下土壤中黄钾铁矾对锑的固持效应研究

冉毅媛[1,2],李学先[1,2],李玲[3],吴攀[1,2,*]

1. 贵州大学资源与环境工程学院,贵阳 550025
2. 喀斯特地质资源与环境教育部重点实验室(贵州大学),贵阳 550025
3. 中国科学院地球化学研究所环境地球化学国家重点实验室,贵阳 550081

摘要:锑矿采冶常导致周边土壤及水体中锑(Sb)的污染,控制污染物Sb向水土环境中迁移对当地的生态环境保护至关重要.黄钾铁矾是一种羟基硫酸盐铁矿物,广泛存在于富含硫酸盐的酸性氧化环境中,对重(类)金属有较好的固定作用.以贵州省Sb矿冶炼厂周边受Sb污染的土壤为研究对象,通过模拟降雨条件下的土柱实验,探究污染土壤剖面中Sb在垂向上的迁移转化特征以及黄钾铁矾对污染土壤中Sb的固持效果.结果表明:降雨前期(0~50 h),有黄钾铁矾土柱中Sb的溶出浓度为20 μg·L^{-1},远低于无黄钾铁矾土柱(70 μg·L^{-1}),黄钾铁矾对Sb的固持效率达到71.4%.模拟降雨后,土壤Sb在土柱剖面发生了垂向迁移,但无黄钾铁矾土柱在5 cm处Sb含量达71.4 mg·kg^{-1},可提取态Sb(可提取态Sb指Wenzel提取法得到的非专性吸附态(F1)+专性吸附态(F2)+无定型铁铝氧化物结合态(F3)+结晶铁铝氧化物结合态(F4))占比较高,Sb有向深层土壤迁移的趋势;而有黄钾铁矾土柱4 cm处Sb含量即达到75.3 mg·kg^{-1},而6 cm处降低为17.2 mg·kg^{-1},可提取态Sb随着土壤深度的增加向更稳定的赋存形态(残渣态(F5))转化,6 cm处可提取态Sb的转化比率达到55.3%,说明黄钾铁矾矿物的添加对Sb的迁移起到固持效果.XPS结果显示,有黄钾铁矾土柱中Fe(II)促进了Fe-O-Sb键的形成,使Fe 2p3/2峰向更高的结合能位点偏移,更接近Fe-Sb共沉淀的结合能位点,土壤中出现Fe-Sb的结合.同时,降雨50 h后,雨水在土柱表层蓄积,Sb溶出浓度增加,表明土壤条件的改变可影响黄钾铁矾的固持效果.

关键词:锑(Sb);黄钾铁矾;模拟降雨;迁移转化

文章编号:0253-2468(2024)09-0347-09　　**中图分类号**:X131.3　　**文献标识码**:A

Antimony retention characteristics of jarosite in soil under simulated rainfall

RAN Yiyuan[1,2], LI Xuexian[1,2], LI Ling[3], WU Pan[1,2,*]

1. College of Resources and Environmental Engineering, Guizhou University, Guiyang 550025
2. Key Laboratory of Karst Georesources and Environment, Ministry of Education, Guiyang 550025
3. State Key Laboratory of Environmental Geochemistry, Institute of Geochemistry, Chinese Academy of Sciences, Guiyang 550081

Abstract: Antimony (Sb) pollution in the surrounding soil and water is often caused by the mining and smelting area. It is very important to control the migration of Sb to soil and water environment for local ecological environment protection. Antimony mining often leads to antimony (Sb) pollution in the surrounding soil and water. It is crucial to control the migration of Sb into soil and water environment for local ecological environment protection. Jarosite is a kind of hydroxyl sulfate iron mineral, which exists widely in acidic oxidation environment rich in sulfate, and has good fixation effect on heavy metals. Taking the soil contaminated by antimony around the Sb mine smelter in Guizhou Province as the object. The vertical migration and transformation characteristics of Sb in contaminated soil profile and the retention effect of jarosite on Sb in polluted soil are investigated by soil column experiments under simulated rainfall conditions. The results show that, in the early period of rainfall (0~50 h), the dissolution concentration of Sb in the column was 20 μg·L^{-1}, much lower than that in the column without jarosite (70 μg·L^{-1}), and the holding efficiency of Sb by jarosite reaches 71.4%. After simulated rainfall, the vertical migration of Sb occurred, however the content of Sb reached 71.4 mg·kg^{-1} at 5cm in the column without jarosite. The extractable Sb (refers to the non-specifically sorbed (F1) + specifically-sorbed (F2) + amorphous and poorly-crystalline hydrous oxides of Fe and Al (F3) + well-crystallized hydrous oxides of Fe and Al (F4) by Wenzel extraction method) accounted for a relatively high proportion, and Sb had a tendency to migrate to deep soil. In the jarosite column, Sb content reached 75.3 mg·kg^{-1} at 4cm, and decreased to 17.2 mg·kg^{-1} at 6 cm. The extractable Sb transformed to a more stable occurrence form (residual state (F5)) with the increase of soil depth, and the conversion ratio of extractable Sb at 6 cm reached 55.3%, indicating that the addition of jarosite minerals had a stabilizing effect on the migration of Sb. XPS results show that Fe(II) promoted the formation of Fe-O-Sb bond in jarosite columns, and the Fe 2p3/2 peak shifted to a higher binding energy, closer to the

收稿日期:2024-01-31　　**修回日期**:2024-03-17　　**录用日期**:2024-03-18
基金项目:贵州省科技计划项目(No.黔科合支撑[2022]一般222;黔科合平台人才-GCC[2023]045);国家重点研发计划(No.2020YFC1807601)
作者简介:冉毅媛(1998—),女,E-mail:1075487525@qq.com; * **责任作者**,E-mail: pwu@gzu.edu.cn

binding energy of Fe-Sb co-precipitation, and Fe-Sb binding appeared in the soil. At the same time, 50 h after rainfall, rainwater accumulated on the surface of column, and the dissolved concentration of Sb increased, indicated that the change of soil conditions can affect the retention effect of jarosite.
Keywords: antimony (Sb); jarosite; simulated rainfall; migration and transformation

1 引言 (Introduction)

锑(Sb)是具有环境危害的类金属元素,被欧盟列入主要的环境污染物(Radková *et al.*, 2023). 辉锑矿(Sb_2S_3)是Sb在矿物中的主要存在形式,Sb在大气、水体和土壤中则主要以+3价$Sb(OH)_3$与+5价$Sb(OH)_6^-$的形式存在(Wilson *et al.*, 2010). 环境中的Sb来源分为自然来源和人为来源,其中,自然来源包括岩石风化成土、生物活动和火山喷发等,人为来源包括Sb矿的开采冶炼、Sb产品的使用和废物焚烧(Månsson *et al.*, 2009; Li *et al.*, 2023). 工业、医药业与制造业对Sb的大量需求促进了Sb矿的采冶,导致环境中Sb含量急剧增加(Robinson, 2009).

中国是Sb的生产大国,产能约占全球的84%(He *et al.*, 2012),长期的Sb生产和使用,导致大量Sb等污染物进入到环境介质中,对环境及人体健康造成的危害也逐渐凸显出来(Bai *et al.*, 2022; Bolan *et al.*, 2022). 西南地区是Sb成矿带的主要分布地(Chen *et al.*, 1991),拥有众多大小型规模不等的Sb矿开采冶炼厂,Sb矿开采和冶炼过程中产生的"三废"进入周围环境,导致矿区周边土壤Sb含量增加,形成Sb污染土壤(Sheng *et al.*, 2022; Gong *et al.*, 2023),且污染时间长、污染风险高(Drahota *et al.*, 2023). 研究显示,湖南锡矿山附近农用地土壤中Sb含量高达400 mg·kg^{-1}(Jia *et al.*, 2022),贵州独山Sb冶炼厂周边农田土壤Sb含量达到98 mg·kg^{-1}(熊佳等, 2020),广西河池Sb冶炼厂周边农用地土壤Sb含量达到300 mg·kg^{-1}(项萌等, 2012),可见Sb矿的开采冶炼已对周围土壤造成不同程度的Sb污染. 此外,有研究也关注了Sb矿区降雨对土壤中Sb迁移及下渗的影响,Long等(2022)采用湖南锡矿山0~20 cm农用地土壤(Sb含量145 mg·kg^{-1})进行模拟酸雨土柱试验,结果显示在模拟pH为2.5的酸雨条件下,渗滤液中Sb的浓度达到2.18 mg·L^{-1},说明Sb在土壤中存在一定的迁移风险. 此外,也有大量研究显示受Sb持久污染的土壤不仅会对地下水产生潜在威胁,同时对植物生长和人类健康也具有潜在危害(Wu *et al.*, 2019; Guo *et al.*, 2021; Vidya *et al.*, 2022). 因此,关注受污染土壤中Sb的迁移对于区域生态环境安全具有重要意义.

土壤中的Sb在降雨淋滤作用下进行垂直向下迁移,在此过程中主要受土壤铁氧化物、锰氧化物、有机质等的影响,将污染物固定在土壤中,或经过吸附解吸等化学反应进一步向周围环境迁移(Zhang *et al.*, 2014; Cai *et al.*, 2016). Sb在土壤中迁移产生的影响已受到研究学者的广泛关注(Sundar *et al.*, 2010; Liu *et al.*, 2011),为实现对土壤中Sb的固定,铁锰氧化物、粘土矿物、有机质、生物炭等材料在Sb污染土壤中被广泛应用(Long *et al.*, 2020; Shi *et al.*, 2021). Jiang等(2023)研究的铁改性蒙脱石对污染土壤中Sb、As、Pb的稳定效率实验中,以土壤/改性材料质量比为10∶1制备土柱,开展淋滤实验,得到处理组对Sb的稳定效率达到86%; Okkenhaug等(2013)探究的添加土壤稳定剂对Sb的稳定效果实验中,按土壤干重2%的比例添加稳定剂制备了土柱,得到添加材料组土柱对Sb的稳定效率达到89%~98%的结果. 黄钾铁矾是锑矿区矿井、水坑、河流中形成的次生羟基硫酸盐铁矿物,也是冶金工业的副产品,其具有多交换位点的化学式能发生多种阴离子和阳离子取代反应,是重要的Sb吸持固定矿物(Bigham *et al.*, 2000; Welch *et al.*, 2007; Johnston *et al.*, 2011). 研究发现,在pH为3的体系中,黄钾铁矾对Sb的吸附使Sb的溶出量减少了大约50%(Karimian *et al.*, 2023). 黄钾铁矾对Sb的吸附机制主要为Sb在其表面形成类似双齿角共享配合物的沉淀,以及通过取代其结构上的Fe,进而与黄钾铁矾结合(Hudson-Edwards, 2019; Karimian *et al.*, 2023),因此,黄钾铁矾对Sb有良好的吸附效果. 对比其它水铁矿、针铁矿、赤铁矿等铁氧化物吸附材料,黄钾铁矾是一种新型有效的吸附Sb的经济性材料(Pappu *et al.*, 2006).

然而,黄钾铁矾对Sb的吸附固定研究多关注于水相,很少有对土壤中Sb的固定研究,有关黄钾铁矾对土壤中Sb迁移转化的影响知之甚少. 因此,本文在模拟降雨条件下,对比添加和未添加黄钾铁矾对土壤中Sb迁移转化的影响,探究Sb在土壤剖面中的垂直迁移特征以及黄钾铁矾对土壤Sb的吸附固定效果,以期为锑矿污染区土壤中Sb的迁移风险评估提供支撑.

2　材料与方法(Materials and methods)

2.1　供试土壤和黄钾铁矾矿物

供试土壤采集自贵州省黔南布依族苗族自治州独山县小河村,土壤剖面样品采集分为两层:表层土壤(0~20 cm),表下层土壤(20~40 cm),土壤质地为壤粘土.表层和表下层土壤pH分别为7.9和7.5,含水率分别为19.5%和15.8%,有机质含量分别为3.25%和0.90%.表层和深层土壤Sb含量分别为65.5 mg·kg^{-1}和17.2 mg·kg^{-1},根据当地土壤Sb背景值(20.6 mg·kg^{-1})和贵州省土壤Sb背景值(2.24 mg·kg^{-1}),说明所采集土壤样品存在Sb污染.

黄钾铁矾($KFe_3(SO_4)_2(OH)_6$)由K、Fe、S、H、O元素组成.实验室用氢氧化钾(KOH)和硫酸铁($Fe(SO_4)_3\cdot 5H_2O$)两种药品制备(Karimian *et al.*, 2023):①将112 g KOH和344.2 g $Fe(SO_4)_3\cdot 5H_2O$(分析级)溶解到2 L超纯水中;②用磁力搅拌器在95 ℃条件下搅拌4 h;③4 h后静置沉淀,倒掉上清液,加入超纯水搅拌洗涤;④重复5次搅拌洗涤步骤;洗涤完成后,将沉淀物放入烘箱中于40 ℃烘干.烘干后的固体过200目筛,取少量用X射线衍射(XRD)表征合成矿物的矿物学形态.制得的黄钾铁矾矿物在XRD中呈现的峰值与黄钾铁矾标准峰对应,无其它杂峰出现.

2.2　土柱模拟实验

2.2.1　土柱装填　实验采用圆形柱填土,圆柱直径6 cm,高20 cm.设定两组模拟降雨条件下的淋滤实验(图1),一组填入过60目筛的表层与深层土壤(对照组),另一组将200目黄钾铁矾和表层土壤以1∶10的质量比均匀混合后填入柱子内(处理组).分别制作3个对照组与3个处理组土柱,作为实验的平行样.将柱子用超纯水洗净风干后,在柱底部铺上石英砂并放置一层棉花,防止土壤样品流失;在柱子侧壁涂抹一层凡士林避免优先流.土样按层位铺入柱子内,每层土壤约180 g,填充深度约5 cm.装填完毕后,在土壤顶部铺设一层石英砂,以使模拟雨水均匀入渗.使用蠕动泵自下而上缓慢泵入0.1 mmol·L^{-1} NaCl水溶液饱和土柱,排出孔隙内空气,待土壤饱和后,改变蠕动泵输水方向,将模拟雨水自土柱上方泵入.

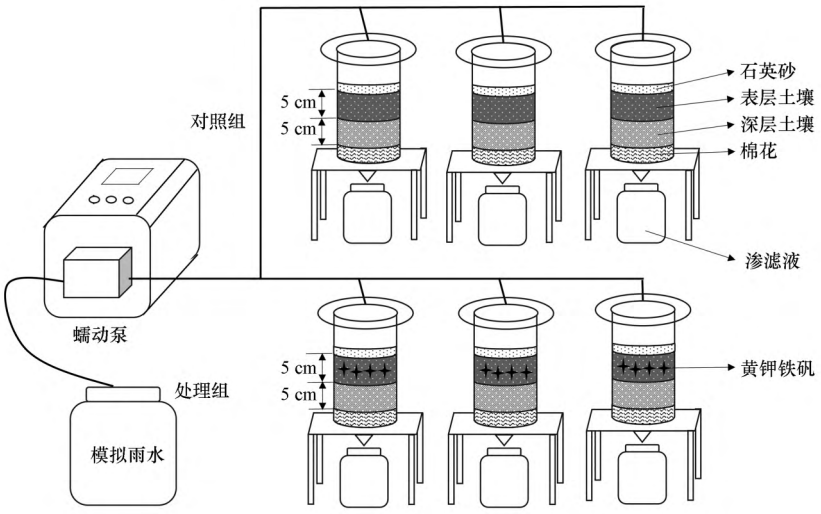

图1　土柱模拟降雨实验

Fig.1　Soil column simulated rainfall experiment

2.2.2　土柱穿透实验　本研究以溴(Br)元素作为土柱穿透实验使用的化学示踪剂开展土柱穿透实验.蠕动泵以0.2 mL·min^{-1}的速度将180 mL 0.1 mmol·L^{-1} KBr溶液缓慢泵入土柱中,随后以相同速度泵入不含KBr的模拟雨水,每30 min收集土柱底部渗滤液.使用电感耦合等离子质谱仪(ICP-MS)检测渗滤液中Br^-浓度.

2.2.3　模拟降雨实验　模拟的雨水组成按照当地的雨水主要成分配备,使用分析级试剂固体$CaCl_2$溶于超纯水制备0.03 mmol·L^{-1} $CaCl_2$溶液(Hou *et al.*, 2013),pH为6.54.模拟降雨实验与穿透实验同步进行:开始供水的前3 d,KBr溶液和模拟雨水同时泵入,泵速为0.2 mL·min^{-1},供水速度为60 mL·d^{-1},每天供水5 h,为间歇式

降雨;3 d后,每天泵入0.03 mmol·L^{-1} $CaCl_2$模拟雨水.前6 d每30 min收集一次底部渗滤液,检测Br^-浓度的变化.6 d后,每天收集一次底部出水口渗滤液,检测Sb溶出浓度的变化.泵入的模拟雨水总量为1200 mL,接近研究区6—9月多雨时期的平均降雨量.每次收集的出水口淋滤液过0.45 μm滤膜后加入1%硝酸并放入4 ℃冷藏室保存.完成降雨实验后,将土柱内的土壤每隔1 cm取出,放入冷冻干燥机干燥24 h,过200目筛后测定土壤物理化学性质,测定方法与2.3节中所述方法一致.

2.3 样品处理与测试

土壤pH使用pH玻璃电极测定.矿物学组成由X射线衍射(XRD,BRUKER D8 ADVANCE,德国)扫描测定.水浴消解-原子荧光法(GB/T 22105.2-2008)测定土壤中的Sb的总量.采用X射线光电子能谱(XPS,Thermo Scientific Nexca)表征土壤固相近表面Fe的化学态.采用Wenzel连续提取法(表1)对土壤中Sb结合态(非专性吸附态、专性吸附态、无定型铁铝氧化物结合态、晶质铁铝氧化物结合态、残渣态)进行逐级提取(Wenzel *et al.*,2001),使用原子荧光光度计测定Sb结合态含量.其中,可提取态Sb的组成为F1+F2+F3+F4,即非专性吸附态(F1)+专性吸附态(F2)+无定型铁铝氧化物结合态(F3)+结晶铁铝氧化物结合态(F4)的统称.

表1 Wenzel顺序提取法对Sb的提取步骤(Wenzel *et al.*, 2001)

Table 1 Wenzel sequential extraction method for Sb extraction steps

Sb结合态		提取条件	水土比
	非专性吸附态(F1)	0.05 mol·L^{-1} $(NH_4)_2SO_4$,25 ℃,振荡4 h	25∶1
可提取态(F1+F2+F3+F4)	专性吸附态(F2)	0.05 mol·L^{-1} $(NH_4)_2PO_4$,25 ℃,振荡4 h	25∶1
(刘冠男等, 2018)	无定型铁铝氧化物结合态(F3)	0.2 mol·L^{-1}草酸铵(pH=3),25 ℃,振荡4 h	25∶1
	结晶铁铝氧化物结合态(F4)	0.2 mol·L^{-1}草酸铵+0.1 mol·L^{-1}抗坏血酸, 96 ℃,振荡30 min	25∶1
残渣态(F5)		王水水浴消解法	\

3 结果与讨论(Results and discussion)

3.1 模拟降雨穿透曲线特征与渗滤液Sb浓度

土柱Br^-穿透曲线见图2a.对照组出水口Br^-浓度达到初始浓度水平,处理组出水口Br^-的峰值浓度达到初始浓度的92%,两组土柱穿透曲线表明土壤样品填充相对均匀(Javaid, 2020).

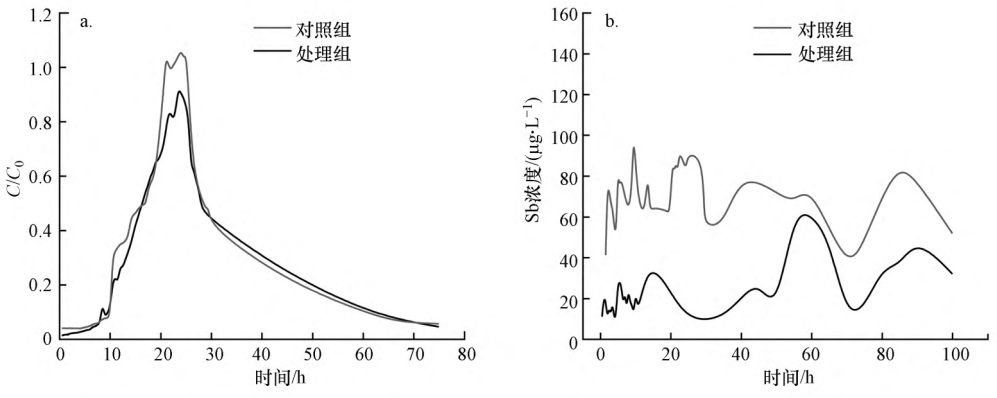

图2 淋滤浓度变化(a. Br^-穿透曲线;b. 模拟降雨过程Sb浓度变化)

Fig.2 Leaching concentration change(a.Br^- breakthrough curve; b.the change of Sb concentration during simulated rainfall)

如图2b所示,Sb的溶出浓度受间歇式降雨的影响而波动.对照组Sb的溶出浓度相对较高,在40~100 μg·L^{-1}的区间波动,平均溶出浓度为70 μg·L^{-1};处理组Sb的溶出浓度较低,在10~40 μg·L^{-1}的区间波动,平均溶出浓度为20 μg·L^{-1},说明黄钾铁矾能够有效抑制污染土壤中Sb的溶出.但在降雨后期(50 h后),处理组Sb的溶出浓度较高,可达60 μg·L^{-1},原因可能是该时期土壤处于蓄水状态,导致Sb的溶出浓度增加(Pan *et al.*, 2016;Johnston *et al.*, 2020).实验用土壤采自锑冶炼厂旁耕地,质地为壤粘土,结合当地降雨量多为小到中雨

的特征(刘相等,2023),耕地土壤不会出现长期积水的极端现象.基于本研究的实验结果,认为添加黄钾铁矾对Sb污染土壤具有一定的固定作用,有实际应用价值.

3.2　模拟降雨前后土壤pH变化

模拟降雨后,土壤pH随深度变化的曲线如图3所示.对照组表层土壤pH从7.84降低到7.13,低于降雨前pH值7.9,这是由于雨水侵蚀表层土壤,表层土壤的pH值降低(Ma *et al.*, 2021).处理组表层土壤pH值从6.69降低到6.58,低于对照组.深层土壤中,对照组pH高于降雨前的pH值7.5,而处理组pH相比降雨前更低.制备的黄钾铁矾矿物材料pH值为3.23,说明添加黄钾铁矾能降低土壤剖面的pH值.前人研究显示,在pH为4的环境中,Sb与黄钾铁矾结合为不溶相,当pH为5时,黄钾铁矾结构上的Sb融入到水相(Karimian *et al.*, 2018),当pH为7时,溶液中出现更多的可溶相Sb(Karimian *et al.*, 2017),说明酸性环境中黄钾铁矾对Sb的固持力强.Sowers等(2022)研究发现,在水溶液有氧酸性条件(pH=2.5)下,黄钾铁矾降低了重金属铅的生物可及性至1%,且没有发生矿物相转变.Karimian等(2017)得知,黄钾铁矾在缺氧水溶液环境,pH=7时,亚铁离子会使黄钾铁矾转化形成针铁矿,过程中释放Sb,增加了Sb的迁移性.而pH=8时含Sb黄钾铁矾中Sb的好氧和非生物释放很有限,因为次生的针铁矿、纤铁矿、绿锈等矿物会重新固持释放的Sb(Hudson-Edwards, 2019).如图3所示,黄钾铁矾在处理组土壤pH范围内,会发生矿物相的转变,但富氧环境中次生的矿物仍能固持土壤中的Sb.

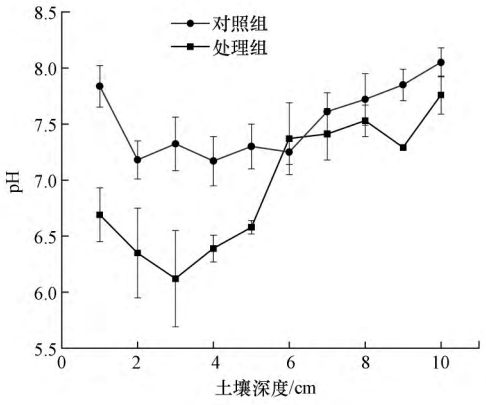

图3　模拟降雨后土壤剖面pH值分布

Fig.3　pH distribution in soil profile after simulated rainfall

3.3　模拟降雨条件下土壤剖面Sb含量变化

模拟降雨实验结束后,土壤剖面每1 cm Sb的总量如图4所示.对照组表层土壤Sb的总量在5 cm处增加到71.4 mg·kg^{-1},高于降雨前Sb的总量65.5 mg·kg^{-1},说明降雨使Sb向下迁移,并在垂直方向上随深度的增加呈现富集特征(Yang *et al.*, 2021),土壤层位交界处富集现象最明显.对照组深层土壤中,Sb在6 cm处含量达到56.8 mg·kg^{-1},远高于降雨前Sb的含量17.2 mg·kg^{-1},表明降雨能够促使Sb向深层土中迁移.

处理组表层土壤Sb的总量变化与对照组不同,Sb在4 cm处富集,总量达到75.3 mg·kg^{-1}.随着深度增加,Sb的富集程度降低,在5 cm处下降到58.6 mg·kg^{-1}.说明降雨条件下,Sb在添加黄钾铁矾的表层土壤中仍会发生垂直迁移,但Sb的富集位置变为土壤层位交界之上的表层土壤中.深层土壤6 cm处Sb的总量远小于对照组,且与降雨前相比无明显变化.结合3.2节的结果可知,土壤中添加黄钾铁矾能减少Sb在垂向上的迁移距离,有效地固持污染物Sb(Courtin-Nomade *et al.*, 2012).

3.4　模拟降雨条件下剖面土壤中Sb赋存形态变化

模拟降雨实验后,Sb的5种结合态含量占比如图5所示.降雨改变了Sb在不同深度土壤中结合态的占比(Pan *et al.*,2021).对照组表层土壤中,可提取态(F1+F2+F3+F4)占比在0~2 cm土层中增加,在2~4 cm土层中保持稳定,5 cm处则有减少(图5b);非专性吸附态(F1)占比则随着土壤深度增加逐渐增加,说明Sb在对照组表层土壤中的迁移能力有所提高,持续增加的非专性吸附态(F1)造成Sb在5 cm处的富集量最高.深层土壤中,6 cm处Sb结合态占比与表层土壤无明显差异,仍有22.2%的非专性吸附态(F1)与52%的可提取态(F1+F2+F3+F4)在该深度中,说明Sb已从表层土迁移到深层土中.

处理组表层土壤可提取态(F1+F2+F3+F4)和非专性吸附态(F1)均小于对照组(图5a、5c).F1向土壤深层的迁移,会对植物根系、土壤微生物的生命活动构成威胁(Du *et al.*,2020).实验结果表明,在土壤中添加黄钾铁矾能够减少可提取态Sb和非专性吸附态Sb,降低Sb在土壤中的迁移能力,对土壤生物的健康威胁更小.深层土壤可提取态Sb的占比随深度的增加持续降低,由23.2%降低到4.1%(图5c),小于对照组由52%降低到6.1%的结果(图5d),说明土壤中添加黄钾铁矾能够阻止Sb的迁移(Palansooriya *et al.*, 2020).

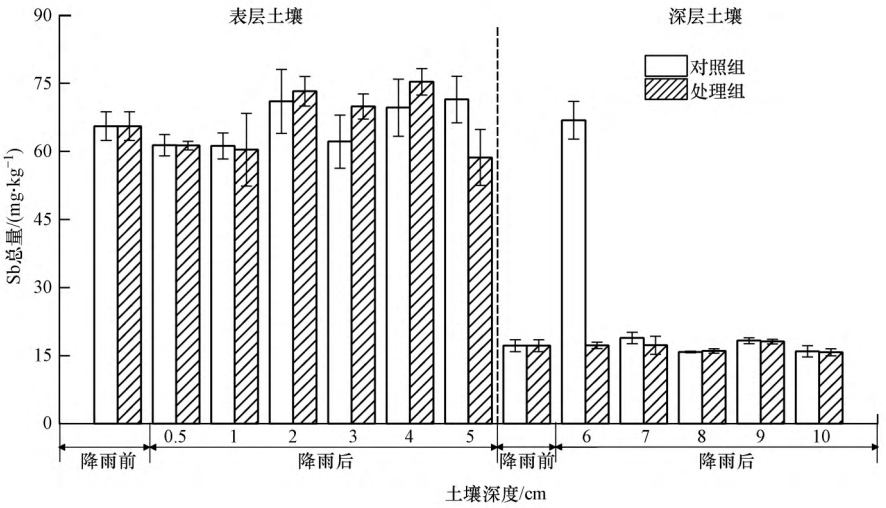

图4 模拟降雨前后Sb总量分布

Fig.4 Total amount of Sb distribution before and after simulated rainfall

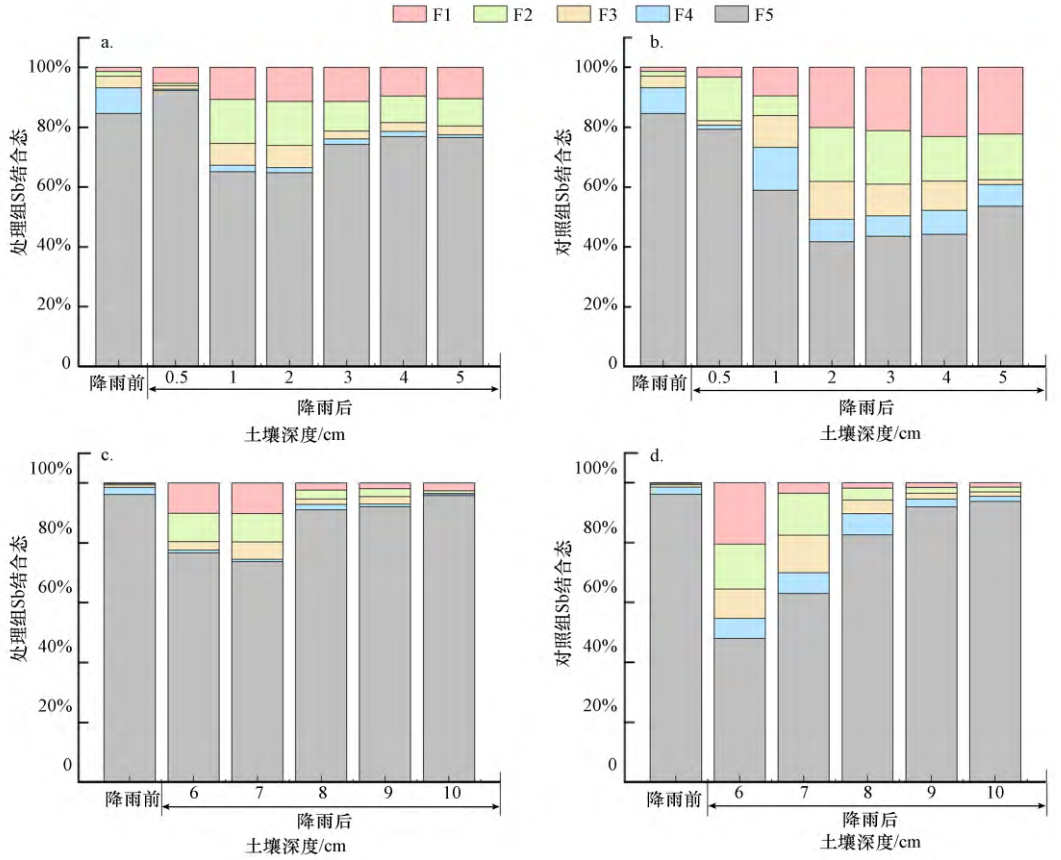

图5 模拟降雨前后土壤表层(0~5 cm)与深层(6~10 cm)Sb结合态分布(a.处理组表层, b.对照组表层, c.处理组深层, d.对照组深层)

Fig.5 Distribution of Sb in surface soil(0~5 cm) and deep soil(6~10 cm) before and after simulated rainfall(a. Surface layer in treatment group, b. Surface layer in control group, c. Deep layer in treatment group, d. Deep layer in control group)

3.5 黄钾铁矾矿物对土壤中Sb迁移影响可能机理

模拟降雨前后,土壤固体表面Fe元素的化学态XPS光谱拟合结果见图6. 702~738 eV的窄谱范围表示Fe 2p. Fe 2p1/2和Fe 2p3/2的结合能点位取决于Fe的氧化态和结晶度(Grosvenor *et al.*, 2004). 当结合能高于710 eV时,Fe以Fe(III)形式存在,结合能小于710 eV时,Fe以Fe(II)形式存在(Jin *et al.*, 2020).

降雨前,Fe(III)结合能分别位于710.1、711.7 、713.6、725.5 eV处,结合能718 eV处为Fe 2p卫星峰(Fan *et al.*, 2019; Fan *et al.*, 2016).降雨后,对照组表层土壤出现结合能为709.7 eV的分峰(图6b),而处理组表层土壤中出现结合能为709.8 eV的分峰,且峰面积为对照组的3.6倍(图6c),说明土壤中的Fe(III)被还原为Fe(II)(Gan *et al.*, 2015),Fe(II)能够促进Fe-O-Sb键的形成、黄钾铁矾的矿物相转变并固持土壤中的Sb(Karimian *et al.*, 2018).处理组Fe(II)的峰面积更高(图6c),说明Fe(II)的催化效果更强,处理组土壤中Sb能与更多的结构位点结合.其次,Sb的吸附能够改变Fe的原子配位模型,使Fe 2p3/2峰向更高的结合能位点偏移(Fan *et al.*, 2016),更接近Fe-Sb共沉淀的结合能位点(Fan *et al.*, 2016).图6c表层和深层土壤均出现Fe(III)的新峰向高结合能位点偏移,表明土壤中出现Fe-Sb的结合,黄钾铁矾对Sb的迁移起到良好的固持效果.

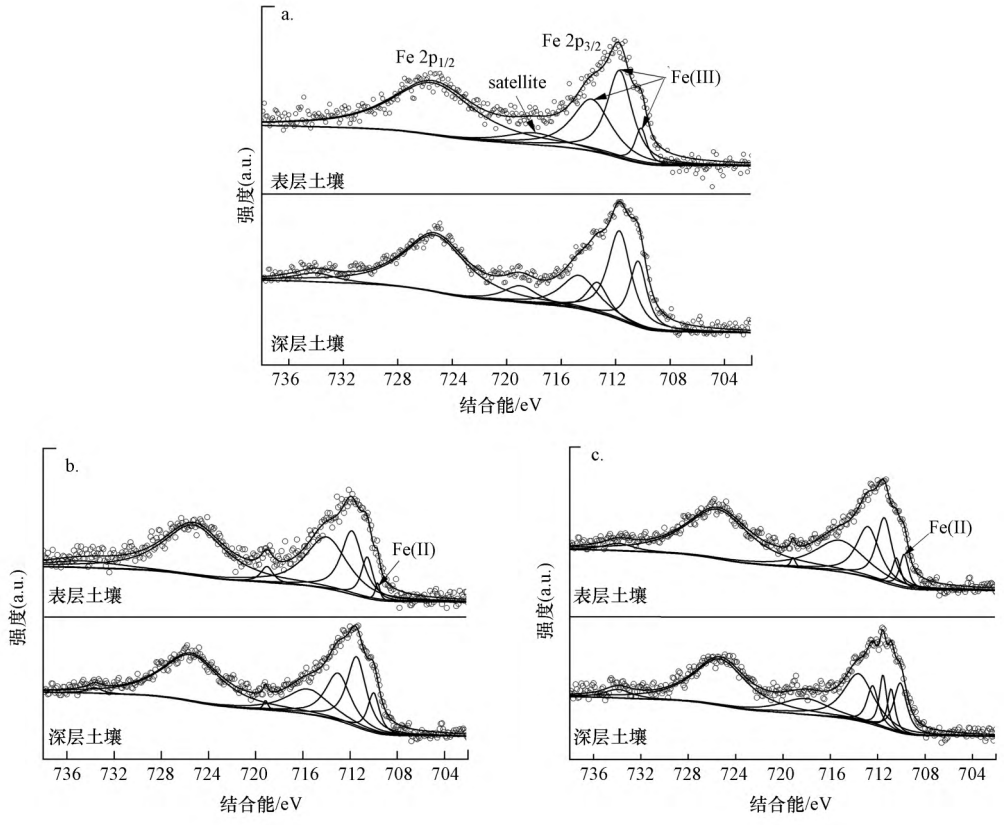

图6　土壤XPS光谱拟合结果(a.模拟降雨前, b.模拟降雨后对照组, c.模拟降雨后处理组)

Fig.6　Fitting results of soil XPS spectra (a.Before simulated rainfall, b.After simulated rainfall in control group, c. After simulated rainfall in treatment group)

4　结论(Conclusions)

1)模拟降雨过程中,对照组与处理组土柱底部渗滤液中均检测到Sb的溶出,但在0~50 h期间,处理组Sb的溶出浓度为20 μg·L^{-1},低于对照组70 μg·L^{-1},黄钾铁矾能够有效抑制污染土壤中Sb的溶出,对Sb的固持效率达到71.4%. 50 h后,土壤条件的改变(由透水变为蓄水)使处理组Sb的溶出浓度增大到60 μg·L^{-1}.实验用土壤质地为壤粘土,结合当地降雨量多为小到中雨的特征,耕地土壤不会出现长期积水的极端现象.基于本研究的实验结果,认为添加黄钾铁矾对Sb污染土壤具有一定的固定作用,有实际应用价值.

2)模拟降雨后对照组6 cm处Sb含量达到56.8 mg·kg^{-1},高于处理组17.2 mg·kg^{-1};可提取态Sb占比为52%,而处理组中占比仅为23.2%,添加黄钾铁矾使6 cm处可提取态Sb向残渣态Sb的转化比率达到55.3%.在降雨作用下,Sb有向深层土壤迁移的趋势,土壤中添加黄钾铁矾能够减少Sb在垂直方向上的迁移量.

3)对照组和处理组表层土壤XPS图中出现结合能为709 eV的新峰,说明降雨导致土壤中Fe(III)被还原为Fe(II),Fe(II)能够促进Fe–O–Sb键的形成;处理组土壤出现新的Fe(III)的拟合峰,出现Fe-Sb结合.在土壤中添加黄钾铁矾对Sb的迁移具有固持效果.

责任作者简介:吴攀,男,教授,博士生导师.从事岩溶地质环境演化、矿山环境污染过程与控制、水/土环境重金属污染与治理修复等研发工作.主持国家重点研发计划课题、国家自然科学基金重大项目(喀斯特科学中心联合基金)等20余项,发表论文140余篇.

参考文献(References):

Bai Z, He Y, Han Z, *et al*.2022.Leaching mechanism and health risk assessment of As and Sb in tailings of typical antimony mines: A case study in Yunnan and Guizhou Province, Southwest China[J].Toxics,10(12):777

Bigham J, Nordstrom D.2000.Iron and aluminum hydroxysulfates from acid sulfate waters[J].Reviews in Mineralogy and Geochemistry,40(1):351-403

Bolan N, Kumar M, Singh E, *et al*.2022.Antimony contamination and its risk management in complex environmental settings: A review[J].Environment International,158:106908

Cai Y, Mi Y, Zhang H J.2016.Kinetic modeling of antimony(III) oxidation and sorption in soils[J].Journal of Hazardous Materials,316:102-109

Chen J, Wei F, Zheng C, *et al*.1991.Background concentrations of elements in soils of China[J].Water, Air, and Soil Pollution,57:699-712

Courtin-Nomade A, Rakotoarisoa O, Bril H, *et al*.2012.Weathering of Sb-rich mining and smelting residues: Insight in solid speciation and soil bacteria toxicity[J].Geochemistry,72:29-39

Drahota P, Venhauerova P, Strnad L.2023.Speciation and mobility of arsenic and antimony in soils and mining wastes from an abandoned Sb-Au mining area[J].Applied Geochemistry,152:105665

Du X, Gao L, Xun Y, *et al*.2020.Comparison of different sequential extraction procedures to identify and estimate bioavailability of arsenic fractions in soil[J].Journal of Soils and Sediments,20(10):3656-3668

Fan C, Guo C, Zeng Y, *et al*.2019.The behavior of chromium and arsenic associated with redox transformation of schwertmannite in AMD environment[J].Chemosphere,222:945-953

Fan J X, Wang Y J, Fan T T, *et al*.2016.Effect of aqueous Fe(II) on Sb(V) sorption on soil and goethite[J].Chemosphere,147:44-51

Gan M, Zheng Z, Sun S, *et al*.2015.The influence of aluminum chloride on biosynthetic schwertmannite and Cu(II)/Cr(VI) adsorption[J].RSC Advances,5(114):94500-94512

Gong Y, Yang S, Chen S, *et al*.2023.Soil microbial responses to simultaneous contamination of antimony and arsenic in the surrounding area of an abandoned antimony smelter in Southwest China[J].Environment International,174:107897

Grosvenor A P, Kobe B A, Biesinger M C, *et al*.2004.Investigation of multiplet splitting of Fe 2p XPS spectra and bonding in iron compounds[J].Surface and Interface Analysis,36(12):1564-1574

Guo W, Zhang Z, Wang H, *et al*.2021.Exposure characteristics of antimony and coexisting arsenic from multi-path exposure in typical antimony mine area[J].Journal of Environmental Management,289:112493

He M, Wang X, Wu F, *et al*.2012.Antimony pollution in China[J].Science of the Total Environment,421:41-50

Hou H, Yao N, Li J, *et al*.2013.Migration and leaching risk of extraneous antimony in three representative soils of China: Lysimeter and batch experiments[J].Chemosphere,93(9):1980-1988

Hudson-Edwards K A.2019.Uptake and release of arsenic and antimony in alunite-jarosite and beudantite group minerals[J].American Mineralogist,104(5):633-640

Javaid M S.2020 Groundwater Hydrology[M].London:IntechOpen

Jia Y, Zhang W, Liu M, *et al*.2022.Spatial distribution, pollution characteristics and source of heavy metals in farmland soils around antimony mine area, Hunan Province[J].Polish Journal of Environmental Studies,31(2):1653-1665

Jiang M, Wang K, Li G, *et al*.2023.Stabilization of arsenic, antimony, and lead in contaminated soil with montmorillonite modified by ferrihydrite: Efficiency and mechanism[J].Chemical Engineering Journal,457:141182

Jin X, Li X, Guo C, *et al*.2020.Fate of oxalic-acid-intervened arsenic during Fe(II)-induced transformation of As(V)-bearing jarosite[J].Science of the Total Environment,719:137311

Johnston S G, Bennett W W, Doriean N, *et al*.2020.Antimony and arsenic speciation, redox-cycling and contrasting mobility in a mining-impacted river system[J].Science of the Total Environment,710:136354

Johnston S G, Keene A F, Bush R T, *et al*.2011.Iron geochemical zonation in a tidally inundated acid sulfate soil wetland[J].Chemical Geology,280(3/4):257-270

Karimian N, Johnston S G, Burton E D.2017.Antimony and arsenic behavior during Fe(II)-Induced transformation of jarosite[J].Environmental Science

& Technology,51(8):4259-4268

Karimian N, Johnston S G, Burton E D.2018.Antimony and arsenic partitioning during Fe^{2+}-induced transformation of jarosite under acidic conditions[J]. Chemosphere,195:515-523

Karimian N, Johnston S G, Tavakkoli E, *et al*.2023.Mechanisms of arsenic and antimony co-sorption onto jarosite: An X-ray absorption spectroscopic study[J].Environmental Science & Technology,57(12):4813-4820

Li X, Sun G, Wu Y, *et al*.2023.Origin and geochemical significance of antimony in Chinese coal[J].International Journal of Coal Geology,265:104165

Liu B J, Wu F C, Li X L, *et al*.2011.Arsenic, antimony and bismuth in human hair from potentially exposed individuals in the vicinity of antimony mines in Southwest China[J].Microchemical Journal,97(1):20-24

刘冠男,陈明,李悟庆,等.2018.土壤中砷的形态及其连续提取方法研究进展[J].农业环境科学学报,37(12):2629-2638

刘相,张宗笛,田人妃,等.2023.贵州6~8月分级降雨气候趋势特征分析[J].内江科技,44(7):81-82

Long J, Tan D, Zhou Y, *et al*.2022.The leaching of antimony and arsenic by simulated acid rain in three soil types from the world's largest antimony mine area[J].Environmental Geochemistry and Health,44(12):4253-4268

Long X, Wang X, Guo X, *et al*.2020.A review of removal technology for antimony in aqueous solution[J].Journal of Environmental Sciences,90:189-204

Ma J, Zhong B, Khan M A, *et al*.2021.Transport of mobile particles in heavy metal contaminated soil with simulated acid rain leaching[J].Bulletin of Environmental Contamination and Toxicology,106(6):965-969

Månsson N S, Hjortenkrans D S, Bergbäck B G, *et al*.2009.Sources of antimony in an urban area[J].Environmental Chemistry,6(2):160-169

Okkenhaug G, Amstätter K, Lassen Bue H, *et al*.2013.Antimony (Sb) contaminated shooting range soil: Sb mobility and immobilization by soil amendments[J].Environmental Science & Technology,47(12):6431-6439

Palansooriya K N, Shaheen S M, Chen S S, *et al*.2020.Soil amendments for immobilization of potentially toxic elements in contaminated soils: A critical review[J].Environment International,134:105046

Pan Y, Bonten L T, Koopmans G F, *et al*.2016.Solubility of trace metals in two contaminated paddy soils exposed to alternating flooding and drainage[J]. Geoderma,261:59-69

Pan Y, Chen J, Gao K, *et al*.2021.Spatial and temporal variations of Cu and Cd mobility and their controlling factors in pore water of contaminated paddy soil under acid mine drainage: A laboratory column study[J].Science of the Total Environment,792:148523

Pappu A, Saxena M, Asolekar S R.2006.Jarosite characteristics and its utilisation potentials[J].Science of the Total Environment,359(1/3):232-243

Radková A B, Jamieson H E, Campbell K M, *et al*.2023.Antimony in mine wastes: geochemistry, mineralogy, and microbiology[J].Economic Geology,118(3):621-637

Robinson B H.2009.E-waste: An assessment of global production and environmental impacts[J].Journal of Environmental Management,408(2):183-191

Sheng L, Hao C, Guan S, *et al*.2022.Spatial distribution, geochemical behaviors and risk assessment of antimony in rivers around the antimony mine of Xikuangshan, Hunan Province, China[J].Water Science and Technology,85(4):1141-1154

Shi M, Min X, Ke Y, *et al*.2021.Recent progress in understanding the mechanism of heavy metals retention by iron (oxyhydr)oxides[J].Science of the Total Environment,752:141930

Sowers T D, Blackmon M D, Bone S E, *et al*.2022.Successful conversion of Pb-contaminated soils to low-bioaccessibility plumbojarosite using potassium-jarosite at ambient temperature[J].Environmental Science & Technology,56(22):15718-15727

Sundar S, Chakravarty J.2010.Antimony toxicity[J].International Journal of Environmental Research and Public Health,7(12):4267-4277

Vidya C S N, Shetty R, Vaculíková M, *et al*.2022.Antimony toxicity in soils and plants, and mechanisms of its alleviation[J].Environmental and Experimental Botany,202:104996

Welch S A, Christy A G, Kirste D, *et al*.2007.Jarosite dissolution I—Trace cation flux in acid sulfate soils[J].Chemical Geology,245(3/4):183-197

Wenzel W W, Kirchbaumer N, Prohaska T, *et al*.2001.Arsenic fractionation in soils using an improved sequential extraction procedure[J].Analytica Chimica Acta,436(2):309-323

Wilson S C, Lockwood P V, Ashley P M, *et al*.2010.The chemistry and behaviour of antimony in the soil environment with comparisons to arsenic: A critical review[J].Environmental Pollution,158(5):1169-1181

Wu T L, Cui X D, Cui P X, *et al*.2019.Speciation and location of arsenic and antimony in rice samples around antimony mining area[J].Environmental Pollution,252:1439-1447

项萌,张国平,李玲,等.2012.广西铅锑矿冶炼区土壤剖面及孔隙水中重金属污染分布规律[J].环境科学,33(1):266-272

熊佳,韩志伟,吴攀,等.2020.独山锑冶炼厂周边土壤锑砷空间分布特征、污染评价及健康风险评估[J].环境科学学报,40(2):655-664

Yang S, Feng W, Wang S, *et al*.2021.Farmland heavy metals can migrate to deep soil at a regional scale: A case study on a wastewater-irrigated area in China[J].Environmental Pollution,281:116977

Zhang H, Li L, Zhou S J.2014.Kinetic modeling of antimony(V) adsorption-desorption and transport in soils[J].Chemosphere,111:434-440